shown in Figures 13 and 14. For the early metamorphic stage I, characterized by the inclusion assemblage of kyanite, dolomite, phengite, (clino)zoisite and omphacite in garnet (Fig. 13), P-T conditions around 2.0 GPa and 660 °C were estimated (Fig. 14). At this stage there should be little garnet present, according to the calculation results (see Table 5). Garnet grew during further burial mainly at the expense of carbonate minerals (dolomite and inferred magnesite), quartz/coesite and zoisite-epidote. Peak P-T conditions (stage II) cannot be precisely assessed as the garnet composition is not very sensitive at the inferred P-T conditions around 4.5 GPa and 1050 °C (see Fig. 14). Zr in rutile geothermometry yielded ca. 900 °C (at 4.5 GPa) based on the calibration by Tomkins et al. (2007) and 19 of 20 rutile analyses with a mean value close to 1300 ppm Zr. Application of the garnet-omphacite Fe^{2+}-Mg exchange thermometry gave temperatures around 1200 °C at 4.5 GPa, using the calibration by Ellis and Green (1979). However, this temperature estimate is rather uncertain, due to the difficulty in determining the amounts of Fe^{2+} and Fe^{3+} in omphacite. The retrograde stage III, which is characterized by micas and kyanite of the matrix and the garnet and omphacite outermost rims (see Table 3), was defined at P-T conditions around 1.6 GPa and 770–800 °C (Fig. 14).

Eclogite E99-24 yielded a $\delta^{13}C$(PDB) value of −9.2 (analytical method as reported by Massonne and Tu, 2007). Such a result for $\delta^{13}C$ does not exclude freshwater carbonates as a possible source of carbon in the protolith of this eclogite. On the other hand, the $\delta^{13}C$ value would still be compatible with mantle carbon (usually around $\delta^{13}C$(PDB) = −5).

Stage	I	II	III
P/GPa	2.1	4.5	1.8
T/°C	670	1050	780
Om	15.3	20.4	42.3
Gt	2.9	55.7	40.4
Zo/Ep	21.3		
Ph	2.8	4.0	4.2
Pa	4.0		
Ky	6.0		6.0
Q/Cs	21.1	12.1	6.1
Rt	0.7	0.9	0.9
Do	9.4	6.8	
Mg	16.4		
XNa(Om)	0.54	0.59	0.30
XCa(Gt)	0.255	0.355	0.29
XFe(Gt)	0.47	0.26	0.345
XMg(Gt)	0.24	0.38	0.36
Si(Ph) pfu	3.30	3.42	3.25

Stages and mineral abbreviations as in Fig. 13.

■ **Tab. 5.** Modal content (in vol%) and compositional characteristics of minerals calculated with the PERPLE_X software for the simplified eclogite composition of E99-24.

Stop 1-3 – B (Day 1). Saidenbachite at the Eastern Shore

Coordinates: N50°44′10.0″ E13°15′08.6″

Walk back along the shore, cross the Saidenbach creek, turn to the south, and continue to walk along the shore until the forest road changes to a westerly direction. Then, continue walking for about 400 metres to some large boulders that, however, would be partially submerged when the reservoir is at its maximum level.

Boulders of saidenbachite differ from those of migmatitic gneisses ("Flammengneise") that occur abundantly as field stones and blocks along the strand and in the adjacent forest. Saidenbachite is a non- or slightly foliated quartzofeldspathic rock with a homogeneous distribution of abundant mm-sized garnets in a muscovite-rich matrix. Boulders of saidenbachite, which are distributed for 500 metres to the west, occur only very locally and are likely related to (lensoid?) bodies underground surrounded by migmatitic gneisses (see map of Fig. 9).

Microdiamonds up to 30 µm, but generally between 5 to 10 µm, in diameter occur as inclusions in garnet and other phases (Fig. 15) of the saidenbachite and were first reported by Massonne (1999). Nasdala and Massonne (2000) confirmed the existence of these microdiamonds by Raman-spectroscopy. Hwang et al. (2001) and Stöckhert et al. (2001) reported the association of quartz, feldspars, various micas, and occasionally apatite and rutile with diamond within a single inclusion in garnet (Fig. 15). These authors interpreted such polyphase inclusions as trapped siliceous fluid or melt. The microdiamonds themselves contain nanometre-sized inclusions, the minerals of which can hardly be identified and related to the larger inclusion minerals (Dobrzhinetskaya et al., 2003).

Detailed studies of saidenbachite demonstrate that the microdiamonds are enclosed in an intermediate compositional zone of garnet (Massonne, 2003) characterized by relatively low Ca concentrations (Table 6, Fig. 16). Microdiamond inclusions also occur in an intermediate zone of mm-sized kyanite grains, which are relicts corroded by potassic white mica (Fig. 17). Occasionally, abundant small idiomorphic garnets are enclosed in the cores of kyanite.

Microdiamonds also occur in an intermediate growth zone in zircon (Fig. 18). Rare inclusions of graphite, garnet and jadeite were found in zircon cores (Nasdala and Massonne, 2000; Massonne and Tu, 2007). In addition, inclusions of phengite, quartz, and rutile occur in garnet cores. From the assemblage of these inclusions, P-T conditions of 1.8 GPa and 650 °C were derived by geothermobarometry (Massonne and Nasdala, 2003) a result which is the same as the peak pressure estimated for gneisses in the vicinity of the saidenbachites (Willner et al., 1997) and for eclogite of stop 1-2 (see Fig. 8). This coincidence

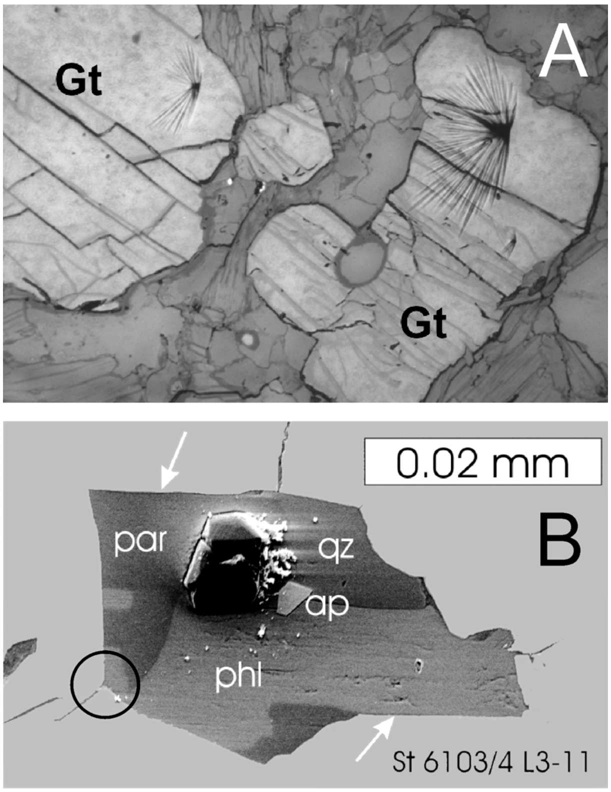

■ **Fig. 15.** (A) Photomicrograph of microdiamonds enclosed in garnet (Gt) from quartzofeldspathic rock E97-3 (alternative stop 1-3E) seen under reflected light. Striations around the diamonds, due to the preparation method applied (Massonne et al., 1998), allow their detection. Image width is 3 mm. (B) SEM image of a polyphase diamond-bearing inclusion in garnet from saidenbachite (Stöckhert et al., 2001). Arrows point to rational mica garnet interfaces. The circle marks an offshoot that typically originated at the edges of such inclusions by decrepitation due to internal overpressure. qz = quartz, par = paragonite, phl = phlogopite, ap = apatite.

was interpreted by Massonne and Nasdala (2003) as evidence for the location of the saidenbachite protolith at the base of a continental crust thickened to 60 km, or more, during the Variscan orogeny. Subsequently, this protolith was deeply buried into the mantle to be heated to about 1200 °C (Massonne, 2003) resulting in extensive anatexis. Corresponding melts, containing residual garnet and zircon (cores), ascended from depths of more than 150 km (the diamond-graphite transition occurs in depths of 150 km at 1100 °C). If TiO_2 with α-PbO_2 structure, found by Hwang et al. (2000) in saidenbachite, would have been a stable phase, this depth could have been 200 km or more. During ascent, still at high pressures, garnet and kyanite, but also rutile, zircon, and diamond, crystallized from the magma (Massonne, 2003). Finally, the magma was emplaced in deep portions of still thickened continental crust at P-T conditions of 1.5 to 1.8 GPa (55–60 km) and temperatures close to 750 °C, as determined by phengite geothermobarometry (Massonne, 1999; 2003). At this stage considerable muscovite formed by a peritectic reaction from the remaining melt (Massonne, 2003) and during subsequent retrogression, some biotite grew at the expense of muscovite. It is noteworthy that several microstructural features indicate the early formation (or existence) of coesite, jadeitic pyroxene, and possibly K-cymrite during the ascent of the saidenbachitic magma (Massonne, 2003; Massonne and Nasdala, 2003).

In contrast to the magmatic interpretation for the genesis of saidenbachite, Hwang et al. (2006) suggested that microdiamonds were generated by infiltration of ultrapotassic fluids. However, the enclosure of abundant small garnet crystals in kyanite (Fig. 17) cannot be explained by such fluid infiltration. On the contrary, crystallization of a saidenbachitic melt can account for this texture by undercooling accompanied by formation of many garnet nuclei (Massonne, 2003). In addition, the concentration of phosphorus in saidenbachite is so low (Tab. 7) that the amounts of the putative “P/K-rich melts”, penetrating and reacting with gneissic rocks as suggested by Hwang et al. (2006), must also be very low. Thus, it would be surprising that such

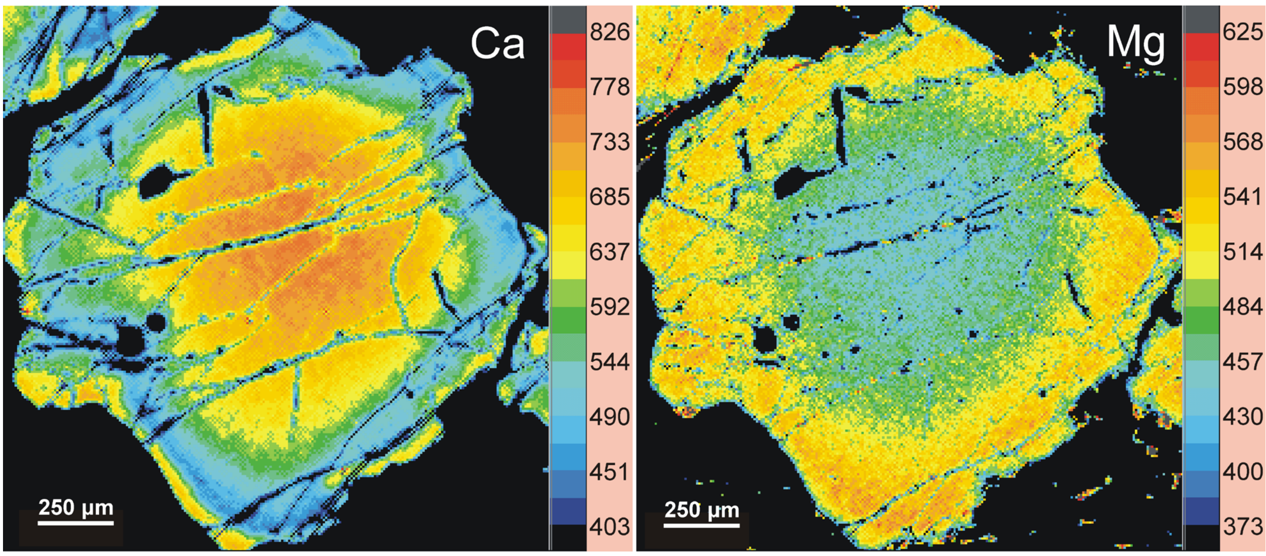

■ **Fig. 16.** Concentration maps of Ca and Mg of garnet in saidenbachite sample E97-2 (alternative stop 1-3E) taken from Massonne and O’Brien (2003).

Mineral	kyanite	garnet core	garnet intermediate zone	garnet rim	garnet core	garnet incl. in zircon	jadeite incl. in zircon	phengite incl. in garnet	phengite core	phengite rim
Sample	E97-2	E97-2	E97-2	E97-2	St6100	St6100	St6100	St6100	E97-1	E97-1
SiO_2	36.66	38.57	38.66	39.00	38.80	39.07	58.54	49.67	47.90	47.15
TiO_2	0.067	0.203	0.133	0.053	0.075	0.018	0.284	3.32	2.11	2.32
Al_2O_3	63.19	22.20	22.32	22.34	22.59	22.44	22.80	28.25	28.64	29.70
Cr_2O_3	0.037	0.02	0.02	0.06	0.01	0.04	0.02	0.05	0.05	0.05
FeO_{tot}	0.084	26.06	26.11	25.32	26.02	24.93	1.72	1.11	1.48	1.54
MnO		0.34	0.34	0.295	0.39	0.25	0.00	0.06	0.00	0.03
MgO	0.046	7.57	8.26	8.33	9.59	10.18	2.28	3.51	2.97	2.59
CaO		5.50	4.40	5.22	3.57	3.44	3.04	0.01	0.02	0.01
Na_2O					0.13	0.08	11.95	0.72	0.27	0.23
K_2O					0.00	0.00	0.00	9.77	9.91	9.91
BaO								0.28	0.32	0.21
F								0.21	0.11	0.10
Total	100.08	100.46	100.24	100.62	101.17	100.44	100.63	96.97	93.79	93.83
Si	0.988	5.906	5.918	5.936	5.785	5.871	2.003	6.497	6.476	6.367
Ti	0.0014	0.024	0.016	0.006	0.008	0.002	0.007	0.327	0.215	0.235
Al	2.007	4.006	4.026	4.006	3.970	3.974	0.920	4.354	4.564	4.727
Cr	0.0008	0.002	0.002	0.006	0.001	0.004	0.001	0.005	0.005	0.005
Fe	0.0019	3.338	3.342	3.220	3.245	3.133	0.049	0.122	0.167	0.174
Mn		0.044	0.044	0.038	0.049	0.032		0.006	0.000	0.004
Mg	0.0019	1.728	1.884	1.890	2.131	2.280	0.116	0.685	0.598	0.521
Ca		0.902	0.720	0.850	0.570	0.554	0.111	0.001	0.000	0.000
Na					0.035	0.022	0.793	0.184	0.070	0.060
K									1.710	1.706
Ba									0.017	0.011
F								1.645	0.048	0.044

■ **Tab. 6.** Electron microprobe analyses (in wt.%) of minerals in diamondiferous quartzofeldspathic rocks from the Saidenbach reservoir taken from Massonne (1999) and Massonne and Nasdala (2003). Structural formulae were calculated as given in Table 4.

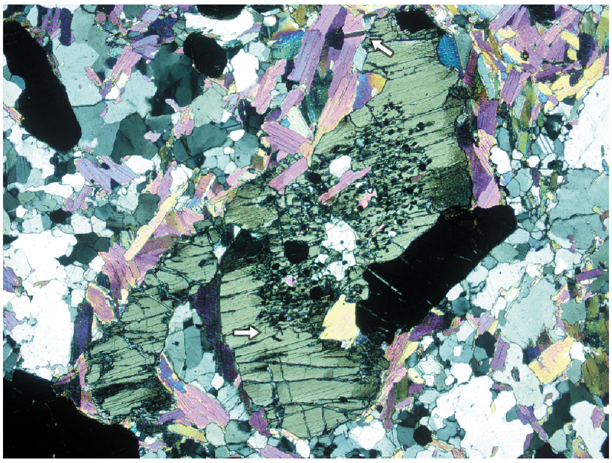

■ **Fig. 17.** Photomicrograph of a large kyanite from sample E97-3 (alternative stop 1-3E), viewed under crossed nicols (Massonne, 2003). The colour image was taken from Massonne and O'Brien (2003). Kyanite is partly replaced mainly by micas. Abundant small garnets are enclosed in the core of the crystal. Arrows point to enclosed microdiamonds. Image width is 4 mm.

small amounts of penetrating fluids could produce abundant polyphase inclusions in mm-scale garnet sometimes throughout a nearly entire garnet grain (Stöckhert et al., 2009).

The various metamorphic-magmatic stages were dated by SHRIMP analysis of Pb, U, and Th isotopes in zircon (Massonne et al., 2007). The determined ages were around 337 Ma (Fig. 19) for core and intermediate domains of zircon (see Fig. 18). Zircon rims yielded a mean age of 330 Ma. In addition, monazite ages from SHRIMP and electron microprobe analyses were about 332 Ma and 325 Ma, respectively (Massonne et al., 2007). Monazite appears exclusively in the matrix of the saidenbachites and is a relatively late-stage mineral. Based on such U-Th-Pb dating results and the above described P-T path, Massonne et al. (2007) estimated that burial rates for the saidenbachites and their protoliths were on the order of several cm per year, and that exhumation rates were »10 cm per year (Fig. 19). This very high exhumation rate was explained by ascent of the saidenbachitic magma, from which the intermediate zircon domain crystallized. This view is supported by Stöckhert et al. (2009), who deduced a minimum exhumation rate on the order of 100 m per year, based on decrepitation of fluid inclusions in garnet (see Fig. 15B), rather than plastic deformation of the enclosing garnet.

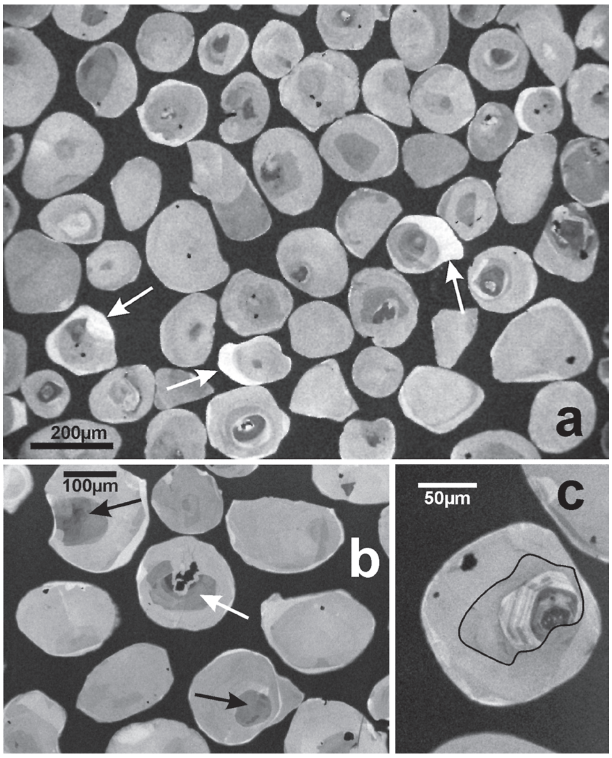

■ **Fig. 18.** Cathodoluminescence (CL) images of zircon grains (fraction 125-250 µm) separated from saidenbachite sample St6100 (alternative stop 1-3E). These images were taken from Massonne et al. (2007). (a) Overview. White arrows show relatively extended zircon rims with light CL. Less than half of the grains show cores with minor CL. Black spots in the zircons are due to mineral inclusions, among which microdiamonds dominate. (b) Enlarged area of the zircon population. Arrows show zircon cores which are typically corroded. This is shown best in the middle zircon (white arrow), where relatively large microdiamonds (black spots) appear. In addition, the diamond-bearing intermediate zone in zircons often shows a relatively homogeneous CL. (c) Zircon with core (tentatively outlined by the black line) showing rare alternating zones typical of magmatic zircons.

	1 E99-2a	2 E00-4	3 E98-7b	4 KD54	5 KD55	6 KD63
SiO_2 in wt.%	64.33	69.77	59.58	74.26	71.12	74.19
TiO_2	0.76	0.61	1.04	0.29	0.42	0.30
Al_2O_3	18.03	15.04	21.56	14.19	14.84	13.29
FeO_{tot}	5.29	4.71	6.29	2.53	2.73	1.94
CaO	0.95	1.46	0.28	1.59	1.33	0.90
MgO	2.46	2.00	1.52	0.89	0.82	0.47
MnO	0.05	0.06	0.05	0.04	0.03	0.02
K_2O	3.39	2.41	5.65	1.77	4.85	5.02
Na_2O	2.51	3.23	0.37	4.28	2.92	2.51
P_2O_5	0.05	0.04	0.07	0.07	0.16	0.18
H_2O_{tot}	1.30	0.58	2.86	0.52	0.56	0.92
CO_2	0.09	0.08	0.04	0.03	0.04	0.05
Sum	99.21	99.99	99.31	100.46	99.82	99.79
Li in ppm	*100.6*	*100.1*	*65.4*	*120.0*	*42.3*	*76.0*
Sc	*20.6*	*15.6*	*6.0*	*9*	*7.2*	*4.9*
V	117	89	139	32	40	25
Cr	77	64	114	1	11	0
Ni	*45.4*	*26.1*	*23.1*	*3.85*	*8.45*	*5.01*
Cu	17	0	19	10	0	5
Zn	104	67	22	31	41	36
Ga	23	19	33	19	18	19
Rb	135	103	338	73	170	252
Sr	*112*	*102.4*	*12.8*	*27*	*112.5*	*94.2*
Y	*13.8*	*14.9*	*10.2*	*65.8*	*45.1*	*49.0*
Zr	167	166	103	83	190	172
Nb	*13.7*	*12.7*	*19.8*	*6.57*	*11.1*	*14.8*
Sn	*1.84*	*2.17*	*34.8*	*8.95*	*2.8*	*4.6*
Ba	415	297	699	142	657	430
Hf/Zr	*0.053*	*0.032*	*0.030*		*0.032*	*0.034*
Ta	*0.92*	*0.92*	*1.92*	*0.25*	*0.61*	*1.44*
Pb	*2.12*	*1.83*	*3.25*	*1.14*	*14.41*	*32.12*
Th	*2.44*	*6.38*	*4.58*	*0.54*	*12.89*	*16.84*
U	*1.23*	*1.82*	*4.30*	*0.10*	*0.77*	*5.42*

■ **Tab. 7.** XRF and ICP-MS (numbers in italics) analyses of quartzofeldspathic rocks from the GEU of the Saxonian Erzgebirge taken from Massonne and Bautsch (2004). 1,2 = saidenbachite from the Saidenbach reservoir, 3 = rock without diamonds, but with aspect similar to saidenbachite, taken northeast of the serpentinite body at Zöblitz, 4 = gneiss unusually rich in Na sampled SW of the village of Forchheim, 5,6 = ordinary gneisses taken close to diamondiferous rocks SW of Forchheim.

The bulk composition of saidenbachite is typical for that of psammopelite (i.e., low P and relatively high Ti, V, Cr, and Ni contents; Table 7), whereas the surrounding migmatitic gneisses were once granitic rocks (Düffels and Massonne, 2001). According to the study by Tichomirowa (2003), the orthogneisses belong to the red-gneiss family (especially Tichomirowa's type A) which is characterized by elongated zircons. These zircons yield ages in the range, 470–500 Ma, which are interpreted as crystallization ages of S-type granitoids. However, zircon rims around older cores crystallized around 340 Ma during the migmatite-forming event (Tichomirowa et al., 2005). Another difference between saidenbachite and surrounding orthogneiss is shown by their REE patterns, in which a significant Eu anomaly occurs in orthogneisses, but is only moderately developed in saidenbachite (Fig. 20). From the above geochemical differences it is concluded that the saidenbachites do not represent country rocks, which were transformed by later metamorphism and deformation.

Microdiamonds from saidenbachite near Forchheim have a high nitrogen aggregation state (Dobrzhinetskaya et al., 2006) and $\delta^{13}C$(PDB) values around –30 ‰ (Massonne and Tu, 2007). A similar $\delta^{13}C$ signature was found for graphite, both that enclosed in zircon cores and that occurring as relatively large flakes in the rock matrix (Massonne and Tu, 2007). Such $\delta^{13}C$(PDB) values were taken to indicate an organic source for the carbon. Combining the ^{13}C signature with concordant U-Pb ages of ca. 400 Ma for rare oscillatory zoned (magmatic) zircon cores (Fig. 18; Massonne et al., 2007) and a psammopelitic bulk-rock composition, Massonne and Tu (2007) hypothesized that the saidenbachites were sediments deposited no earlier than Mid-Devonian time. In addition, it is conceivable that these sediments were turbidites (see bulk-rock compositions of Table 7)

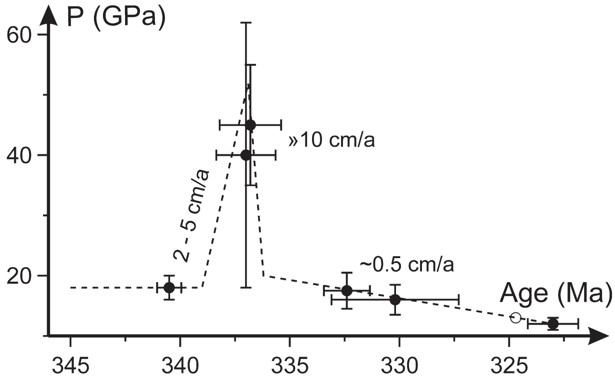

■ **Fig. 19.** Pressure-time diagram displaying a likely burial and exhumation course for saidenbachites from the Saxonian Erzgebirge during an episode of the Variscan orogeny (Massonne et al., 2007). Error bars for time are related to 1σ. The open circle represents the mean age acquired via EMP dating of monazite from saidenbachite by Massonne et al. (2007). The U-Pb zircon age at 340.5 Ma was dated by Kröner and Willner (1998) for sample E42x (at or close to stop 1-3D). The age at 323 Ma is a Rb-Sr biotite (cooling) age determined for a granulite from the nearby Granulitgebirge (see Fig. 1) by Romer and Rötzler (2001) The other ages are SHRIMP U-Pb ages of zircon and monazite from saidenbachite (Massonne et al., 2007).

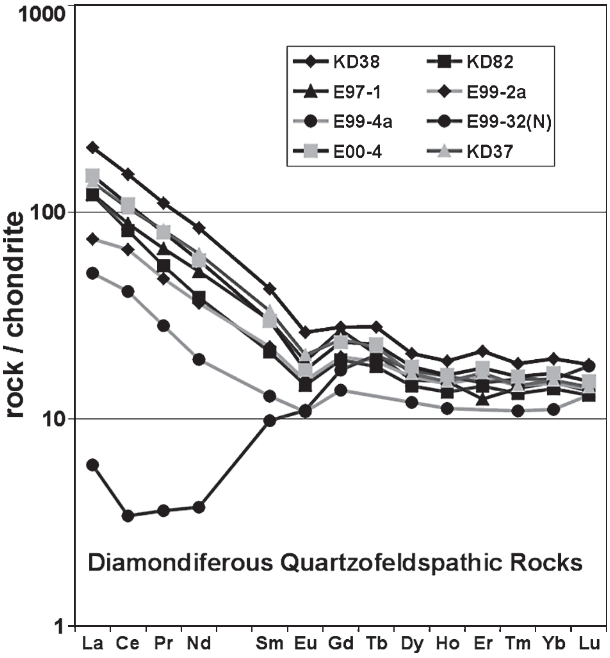

■ **Fig. 20.** REE patterns of saidenbachites from the GEU of the Saxonian Erzgebirge taken from Massonne and Bautsch (2004). The data were obtained by ICP-MS analyses and subsequently normalized to chondrite according to Boynton (1984). The light REE depletion of sample E99-32(N) may be explained by the escape of a melt fraction before complete crystallization. For this reason, monazite is absent from saidenbachite E99-32(N), but present in all other saidenbachites plotted here.

deposited in the shrinking ocean basin before collision of the Laurussia and Gondwana continental plates (or microcontinents derived from Gondwana, e.g., Linnemann et al., 2000)

Subsequently, the protolith of the saidenbachite was likely deeply buried by a subduction event. In this context, Behn et al. (2011) suggested that pelitic material at the top of deeply subducted crust can form buoyant diapirs that ascend into the hot, overlying mantle wedge, where partial melting begins. This scenario may be applicable to the saidenbachites. Alternatively, the saidenbachite characteristics might be related to lithospheric delamination below the thickened Variscan crust, possibly tens of million years after the continent-continent collision (Willner et al., 2002; Massonne, 2005). If crustal material from the base of this thickened crust were already partially (?) eclogitized (see eclogite E174c from stop 1-2 and stage I of eclogite E99-24 from stop 1-3A, and see Leech, 2001), it could have foundered into the hot mantle to be melted there. In either case, buoyant diapirism or crustal delamination, melting of the saidenbachite protolith occurred in the mantle although no interaction with mantle material is discernible in the chemical composition of saidenbachite.

Stop 1-3 – C (Day 1). Eclogite at the Eastern Shore

Coordinates: N50°43′52.5″ E13°14′35.5″

From the western end of the saidenbachite body (stop 1-3B) at the shore of the reservoir, continue walking in a south-westerly direction for 500 metres to a natural outcrop on the shore, which would be still discernible if the water level of the reservoir is at its maximum.

Exposed at this stop (Fig. 9) in the south-eastern portion of the reservoir is a homogeneous eclogite, which is partially penetrated by whitish schlieren and pegmatoid dykes. Thick, up to cm-sized white mica flakes occur in the pegmatoid and such mica also appears in eclogite directly adjacent to the pegmatoid.

The eclogite is characterized by abundant mm-sized garnet grains, which are homogeneously distributed in the rock as in the nearby saidenbachite. The eclogite matrix consists of a greenish-greyish material, which is mainly composed of relatively coarse-grained symplectite of plagioclase, Ca-amphibole and Na-poor clinopyroxene after former omphacite. Although matrix omphacite has been completely altered to symplectite, fresh omphacite has been preserved as relatively large inclusions in garnet (Fig. 21, Table 8) of samples E42-1d and E03-14 from stop 1-3C. This is also true for other natural exposures of this type of homogeneous eclogite along the shore of the Said-